Journal of Organometallic Chemistry, 394 (1990) 711–732
Elsevier Sequoia S.A., Lausanne
JOM 20809

The heteronuclear cluster chemistry of the Group IB metals

XIV *. The influence of the $P(CH_2Ph)_3$ ligand on the metal framework structures adopted by mixed-metal clusters containing $M\{P(CH_2Ph)_3\}$ (M = Cu or Ag) fragments. Crystal structures of $[Cu_2Ru_4(\mu_3\text{-}H)_2(CO)_{12}\{\mu\text{-}P(CH_2Ph)_2(\eta^2\text{-}CH_2Ph)\}]$ and $[Cu_2Ru_4(\mu_3\text{-}H)_2(CO)_{12}\{P(CH_2Ph)_3\}_2]$ **

Carolyn J. Brown, Paul J. McCarthy, Ian D. Salter *
Department of Chemistry, University of Exeter, Exeter EX4 4QD (U.K.)

Kenneth P. Armstrong, Mary McPartlin and Harold R. Powell
School of Chemistry, The Polytechnic of North London, London N7 8DB (U.K.)

(Received January 29th, 1990)

Abstract

Treatment of a dichloromethane solution of the salt $[N(PPh_3)_2]_2[Ru_4(\mu\text{-}H)_2(CO)_{12}]$ with two equivalents of the complex $[M(NCMe)_4]PF_6$ (M = Cu or Ag) at −30 °C, followed by the addition of two equivalents of $P(CH_2Ph)_3$, affords the novel mixed-metal cluster compound $[Cu_2Ru_4(\mu_3\text{-}H)_2(CO)_{12}\{\mu\text{-}P(CH_2Ph)_2(\eta^2\text{-}CH_2Ph)\}]$ (77% yield) when M = Cu, whereas the expected product, $[Ag_2Ru_4(\mu_3\text{-}H)_2(CO)_{12}\{P(CH_2Ph)_3\}_2]$ (37% yield), is obtained for M = Ag. When an acetone solution of $[N(PPh_3)_2]_2[Ru_4(\mu\text{-}H)_2(CO)_{12}]$ is treated with a dichloromethane solution containing two equivalents of the compound $[CuCl\{P(CH_2Ph)_3\}]$, in the presence of $TlPF_6$, a mixture of $[Cu_2Ru_4(\mu_3\text{-}H)_2(CO)_{12}\{\mu\text{-}P(CH_2Ph)_2(\eta^2\text{-}CH_2Ph)\}]$ (44% yield) and $[Cu_2Ru_4(\mu_3\text{-}H)_2(CO)_{12}\{P(CH_2Ph)_3\}_2]$ (12% yield) is produced. Single-crystal X-ray diffraction studies were performed on $[Cu_2Ru_4(\mu_3\text{-}H)_2(CO)_{12}\{\mu\text{-}P(CH_2Ph)_2(\eta^2\text{-}CH_2Ph)\}]$ and $[Cu_2Ru_4(\mu_3\text{-}H)_2(CO)_{12}\{P(CH_2Ph)_3\}_2]$. The former cluster exhibits a capped trigonal bipyramidal metal framework structure (Cu–Cu 2.532(2), Cu–Ru 2.585(2)–2.813(1), Ru–Ru 2.790(1)–2.981(1) Å) and the

* For Part XIII, see ref. 1.

** This paper is dedicated to Professor F.G.A. Stone, F.R.S., on the occasion of his 65th birthday. One of us (I.D.S.) is especially indebted to Professor Stone for the guidance and encouragement given to him while a Ph.D. student.

0022-328X/90/$03.50

single $P(CH_2Ph)_3$ group adopts a novel bidentate bonding mode by bridging the two adjacent copper atoms via bonds from its phosphorus atom (Cu–P 2.199(2) Å) and an η^2-CH_2Ph ring (Cu–C 2.146(10) and 2.339(12) Å). In marked contrast, $[Cu_2Ru_4(\mu_3\text{-}H)_2(CO)_{12}\{P(CH_2Ph)_3\}_2]$ adopts an unusual metal core structure, which consists of a Ru_4 tetrahedron with one edge bridged by a $Cu\{P(CH_2Ph)_3\}$ unit and a non-adjacent face capped by the second $Cu\{P(CH_2Ph)_3\}$ group (Cu–Ru 2.589(4)–2.724(4), Ru–Ru 2.760(3)–2.984(4) Å). Infrared and NMR spectroscopic data show that $[Ag_2Ru_4(\mu_3\text{-}H)_2(CO)_{12}\{P(CH_2Ph)_3\}_2]$ exhibits a capped trigonal bipyramidal skeletal geometry, with the silver atoms in close contact. Thus, although the $P(CH_2Ph)_3$ ligand is evidently too bulky to allow two adjacent $Cu\{P(CH_2Ph)_3\}$ units to be accommodated in the metal skeleton of $[Cu_2Ru_4(\mu_3\text{-}H)_2(CO)_{12}\{P(CH_2Ph)_3\}_2]$, the greater size of the silver atom relative to copper means that the analogous silver-containing species can adopt the metal framework structure which previous work suggests is preferred by clusters of this type. Variable-temperature $^{31}P\text{-}\{^1H\}$ and ^1H NMR spectroscopic studies demonstrate that all three of the new heteronuclear cluster compounds undergo a number of interesting dynamic processes in solution.

Introduction

A wide range of Group IB metal heteronuclear cluster compounds of general formula $[M_2Ru_4(\mu_3\text{-}H)_2(CO)_{12}L_2]$ (I, M = Cu, L = PPh_3; II, M = Cu, L = $PMePh_2$, PMe_2Ph, PEt_3, PMe_3, $P(OPh)_3$, $P(OEt)_3$, or $P(OMe)_3$; III, M = Cu, L = PCy_3 (Cy = cyclo-C_6H_{11}); IV, M = Cu, L = $P(CHMe_2)_3$; V, M = Ag, L = PPh_3; VI, M = Ag, L = $PMePh_2$ or $P(CHMe_2)_3$; VII, M = Ag, L = PCy_3) have now been synthesized [2–6]. These mixed-metal species have all been prepared from the reaction of $[N(PPh_3)_2]_2[Ru_4(\mu\text{-}H)_2(CO)_{12}]$ with two equivalents of $[M(NCMe)_4]PF_6$, followed by the addition of two equivalents of the appropriate phosphorus donor ligand L, and/or by treating the same cluster salt with two equivalents of the complex [MXL] (M = Cu, X = Cl; M = Ag, X = I), in the presence of $TlPF_6$. The preferred skeletal geometry for the clusters of general formula $[M_2Ru_4(\mu_3\text{-}H)_2(CO)_{12}L_2]$ seems to be capped trigonal bipyramidal, with the two Group IB metals in close contact. This is the metal core structure that is observed, in the solid state and in solution, for $[Cu_2Ru_4(\mu_3\text{-}H)_2(CO)_{12}(PPh_3)_2]$ (I) and the series of copper-containing clusters II, in which relatively small phosphine or phospite ligands (cone angles $\leq 145°$ [7]) are attached to the copper atoms [2,3], and also for all of the silver-containing species V–VII [4,5]. However, the bulky phosphine PCy_3 (cone angle 170° [7]) seems to be too large to allow two $Cu(PCy_3)$ units to be adjacent in the metal framework of III and, instead, the cluster exhibits an apparently less favourable skeletal geometry, in which only one Cu atom adopts a face-capping position and the other occupies a sterically less-demanding edge-bridging site [6]. Interestingly, although $[Cu_2Ru_4(\mu_3\text{-}H)_2(CO)_{12}\{P(CHMe_2)_3\}_2]$ (IV) adopts the preferred capped trigonal bipyramidal metal core structure with two adjacent $Cu\{P(CHMe_2)_3\}$ units in the solid state, two skeletal isomers are observed at low temperatures in solution [6]. The skeletal geometry of the more abundant isomer is thought to be the same as that observed for IV in the solid state, but the second isomer probably has two face-capping

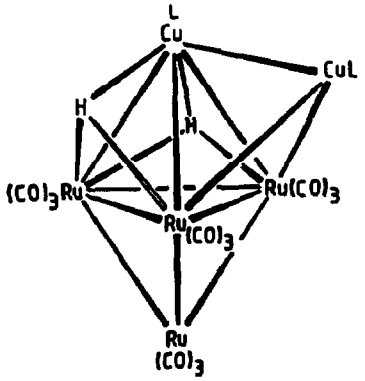

I, L = PPh_3

II, L = $PMePh_2$, PMe_2Ph, PEt_3, PMe_3, $P(OPh)_3$, $P(OEt)_3$, or $P(OMe)_3$

IV, L = $P(CHMe_2)_3$

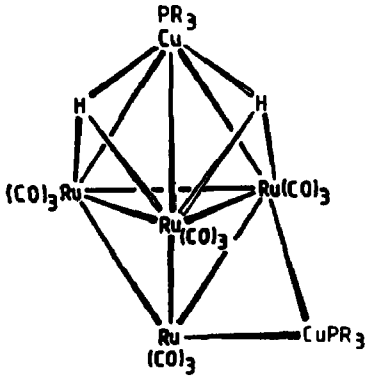

III, R = cyclo-C_6H_{11}

IX, R = CH_2Ph

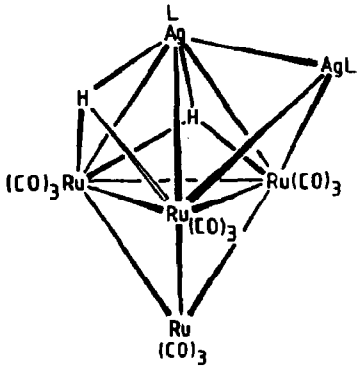

V, L = PPh_3

VI, L = $PMePh_2$ or $P(CHMe_2)_3$

VII, L = $P(cyclo\text{-}C_6H_{11})_3$

X, L = $P(CH_2Ph)_3$

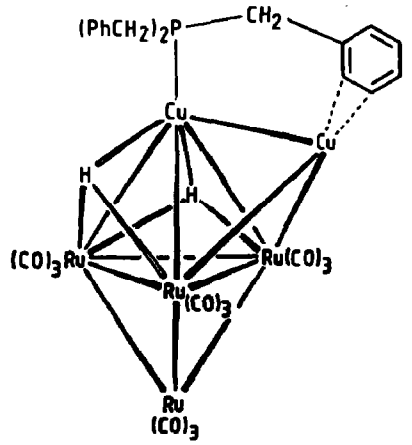

VIII

copper atoms with no bonding interaction between them [6]. Thus, the $P(CHMe_2)_3$ ligand (cone angle 160° [7], which is intermediate between 145° and that of PCy_3) is not sufficiently large to alter the solid state metal core geometry of IV, as observed for the PCy_3 ligand in III, but its steric requirements do influence the structural properties of IV in solution. In view of the interesting results described above, we wished to synthesize analogous clusters containing the $P(CH_2Ph)_3$ ligand, which has a cone angle of 165° [7], intermediate between those of PCy_3 and $P(CHMe_2)_3$, and to investigate their skeletal geometries in the solid state and in

Table 1

Analytical and physical data for the new Group IB metal heteronuclear cluster compounds

Compound	M.pt. (°C) (decomp.)	ν_{max}(CO) (cm^{-1}) [a]	Yield [b] (%)	Analysis (Found (calcd.) (%))	
				C	H
$[Cu_2Ru_4(\mu_3\text{-}H)_2(CO)_{12}\{\mu\text{-}P(CH_2Ph)_2(\eta^2\text{-}CH_2Ph)\}]$ (VIII)	101–104	2071s, 2035vs, 2021vs, 2008s, 1977m br, 1939w br	77	33.7 (33.8)	2.1 (2.0)
$[Cu_2Ru_4(\mu_3\text{-}H)_2(CO)_{12}\{P(CH_2Ph)_3\}_2]$ (IX)	112–116	2065m, 2034vs, 2003vs br, 1947m br, 1930w br, 1908w br	12	43.8 (43.9)	3.0 (3.0)
$[Ag_2Ru_4(\mu_3\text{-}H)_2(CO)_{12}\{P(CH_2Ph)_3\}_2]$ (X)	148–151	2069s, 2031vs, 2019vs, 2003s, 1982m, 1971m, 1940w br	37	41.3 (41.4)	2.8 (2.8)

[a] Measured in dichloromethane solution. [b] Based on ruthenium reactant. When the cluster has been prepared by more than one procedure, the best yield is given.

solution. Preliminary accounts describing some of our results have already been published [8,9].

Results and discussion

Treatment of a dichloromethane solution of the salt $[N(PPh_3)_2]_2[Ru_4(\mu\text{-}H)_2(CO)_{12}]$ with two equivalents of the complex $[Cu(NCMe)_4]PF_6$ at −30 °C, followed by the addition of two equivalents of $P(CH_2Ph)_3$, affords a novel dark red cluster compound, formulated as $[Cu_2Ru_4(\mu_3\text{-}H)_2(CO)_{12}\{P(CH_2Ph)_3\}]$ (VIII) (77% yield) *, instead of the expected product $[Cu_2Ru_4(\mu_3\text{-}H)_2(CO)_{12}\{P(CH_2Ph)_3\}_2]$. The IR spectrum of VIII (Table 1) closely resembles those previously reported [2,3] for the PPh_3-ligated species I and the series of clusters II, suggesting that VIII adopts a similar capped trigonal bipyramidal metal core structure, with the copper atoms in close contact, to those previously established for I and II. Surprisingly, however, the ^1H NMR spectrum of VIII (Table 2) shows a ratio of 1/2 for the signals due to the $P(CH_2Ph)_3$ ligand relative to the hydrido ligand peak, instead of the 2/2 ratio expected from the previous work [2,3], and no other ^1H NMR signals are visible. In view of this unusual result, a single-crystal X-ray diffraction study was performed on VIII.

The molecular structure of VIII is illustrated in Fig. 1 and selected interatomic distances and angles are presented in Tables 3 and 4, respectively. The metal framework of VIII consists of a Ru_4 tetrahedron, with one Ru_3 face (Ru(1)Ru(2)Ru(3)) capped by a copper atom (Cu(1)) and one $CuRu_2$ face (Cu(1)Ru(2)Ru(3)) of the $CuRu_3$ tetrahedron so formed capped by the second copper atom (Cu(2)), so that the two copper atoms are in close contact (Cu(1)–Cu(2) 2.532(2) Å). The single $P(CH_2Ph)_3$ group bridges the Cu–Cu vector by bonding to Cu(1) via its phosphorus atom (Cu(1)–P 2.199(2) Å) and also to Cu(2) via two carbon atoms of a CH_2Ph ring (Cu(2)–C(56) 2.339(12) and Cu(2)–C(57) 2.146(10)

* Similar yields of VIII can be obtained by use of only one equivalent of $P(CH_2Ph)_3$, instead of two.

Table 2

^{1}H and ^{31}P NMR spectroscopic data [a] for the new Group IB metal heteronuclear cluster compounds

Compound	Ambient temperature ^{1}H NMR data [b]	Low temperature ^{1}H NMR hydrido ligand signal [b,c]	Ambient temperature ^{31}P-{^{1}H} NMR data [d]	Low temperature ^{31}P-{^{1}H} NMR data [c,d]
VIII	−18.56 [d, 2H, μ_3-H, J(PH) 12], 3.21 [d, 6H, CH_2Ph, J(PH) 8], 7.22–7.34 (m, 15 H, CH_2Ph)	[e] −18.81 [d br, 2H, J(PH) 12]	16.0 (s vbr)	19.8 (s br)
IX	−16.67 [t br, 2H, μ_3-H, J(PH) 5], 3.09 [d, 12H, CH_2Ph, J(PH) 7], 7.22–7.33 (m, 30H, CH_2Ph)	−17.39 [d br, 1H, J(PH) 9], −15.72, [d, br, 1H, J(PH) 9]	−5.0 (s br)	−5.7 (s br, 1 P), −2.9 (s br, 1 P)
X	[f] −17.22 [overlapping t of t, 2H, μ_3-H, J(AgH)$_{av.}$ 12, J(PH) 5], 2.95 [d br, 12H, CH_2Ph, J(PH) 5] 7.12–7.40 (m, 30H, CH_2Ph)	[g] −17.37 [d of d, 2H, J(AgH)$_{av.}$ 25, J(PH) 8]	[h] 5.0 (m)	[i] 10.9 [2 × d of d, 1 P, J(^{109}AgP) 571, J(^{107}AgP) 495, ^{2}J(AgP)$_{av.}$ 8], −2.0 [2 × d of d, 1 P, J(^{109}AgP) 469, J(^{107}AgP) 406, ^{2}J(AgP)$_{av.}$ 14]

[a] Chemical shifts (δ) in ppm, coupling constants in Hz. [b] Measured in [$^{2}H_2$]dichloromethane solution. [c] Measured at −100 °C, unless otherwise stated. [d] Hydrogen-1 decoupled, measured in [$^{2}H_2$]dichloromethane/CH_2Cl_2 solution, chemical shifts positive to high frequency of 85% H_3PO_4 (external). [e] $P(CH_2Ph)_3$ signals at −100 °C: For the CH_2Ph ring coordinated to copper, δ 3.30 (s br, 2 H, CH_2Ph) and 7.12 (s br, 5 H, CH_2Ph). For the two uncoordinated CH_2Ph rings, δ 3.18 (s br, 4 H, CH_2Ph) and 7.28 (s br, 10 H, CH_2Ph). [f] CH_2 signal at −20 °C: δ 2.90 [d of d, 12 H, J(AgH)$_{av.}$ 3, J(PH) 6]. [g] Measured at −80 °C. [h] The multiplet observed for X consists of superimposed subspectra due to $^{107}Ag^{107}Ag$, $^{107}Ag^{109}Ag$, and $^{109}Ag^{109}Ag$ isotopomers of the cluster and it is complicated by second order effects and by a wide variety of couplings. The pattern of signals in the complex multiplet is very similar to those previously reported [22] in the ambient temperature ^{31}P-{^{1}H} NMR spectra of $[Ag_2Ru_4(\mu_3\text{-}H)_2\{\mu\text{-}Ph_2P(CH_2)_nPPh_2\}(CO)_{12}]$ (n = 4 or 5). However, the energy barriers for the intramolecular metal core rearrangement and the intermolecular phosphine ligand exchange processes that X undergoes in solution are such that it is not possible to obtain a spectrum of X which has narrow enough linewidths to allow all of the peaks that are visible for the $Ph_2P(CH_2)_nPPh_2$-containing species to be fully resolved. Therefore, the values of ^{1}J(^{109}AgP), ^{1}J(^{107}AgP), ^{2}J(^{109}AgP), ^{2}J(^{107}AgP), J($^{109}Ag^{109}Ag$), J($^{109}Ag^{107}Ag$), and J($^{107}Ag^{107}Ag$) cannot be obtained from the spectrum of X using a similar analysis to that previously described [22]. [i] Measured at −90 °C.

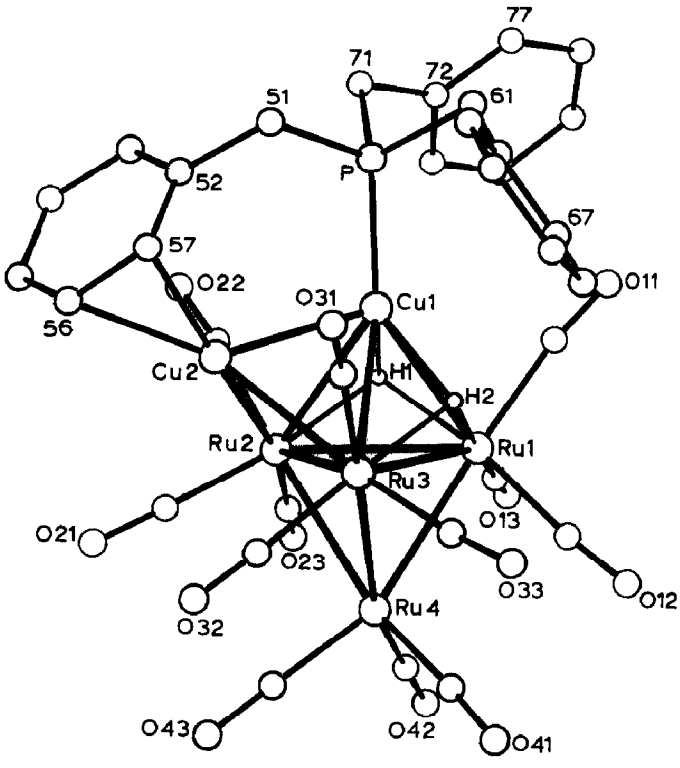

Fig. 1. Molecular structure of $[Cu_2Ru_4(\mu_3\text{-}H)_2(CO)_{12}\{\mu\text{-}P(CH_2Ph)_2(\eta^2\text{-}CH_2Ph)\}]$ (VIII), showing the crystallographic numbering. The carbon atom of each carbonyl group has the same number as the oxygen atom.

Table 3

Selected bond lengths (Å), with estimated standard deviations in parentheses, for $[Cu_2Ru_4(\mu_3\text{-}H)_2(CO)_{12}\{\mu\text{-}P(CH_2Ph)_2(\eta^2\text{-}CH_2Ph)\}]$ (VIII) and $[Cu_2Ru_4(\mu_3\text{-}H)_2(CO)_{12}\{P(CH_2Ph)_3\}_2]$ (IX)

VIII		IX		VIII	IX
Ru(1)–Ru(2)	2.942(1)	2.969(3)	*Ru–C (carbonyl)*		
Ru(1)–Ru(3)	2.981(1)	2.984(4)	range	1.850(12)–1.933(9)	1.82(3)–2.02(6)
Ru(1)–Ru(4)	2.806(1)	2.799(4)	mean	1.892(12)	1.88(3)
Ru(2)–Ru(3)	2.910(1)	2.826(3)	Cu(2)–C (aryl)		
Ru(2)–Ru(4)	2.805(1)	2.760(3)	Cu(2)–C(56)	2.339(12)	–
Ru(3)–Ru(4)	2.790(1)	2.862(3)	Cu(2)–C(57)	2.146(10)	–
Ru(1)–Cu(1)	2.702(1)	2.724(4)	*C–O (carbonyl)*		
Ru(2)–Cu(1)	2.813(1)	2.696(4)	range	1.122(12)–1.189(15)	1.03(6)–1.20(5)
Ru(2)–Cu(2)	2.585(2)	–	mean	1.150(16)	1.15(3)
Ru(3)–Cu(1)	2.717(1)	2.703(5)	C(51)–C(52)	1.525(14)	
Ru(3)–Cu(2)	2.680(1)	2.589(4)	C(52)–C(53)	1.362(13)	
Ru(4)–Cu(2)	–	2.604(4)	C(52)–C(57)	1.413(13)	
Cu(1)–Cu(2)	2.532(2)	–	C(53)–C(54)	1.402(15)	
Cu(1)–P(1)	2.199(2)	2.209(9)	C(54)–C(55)	1.396(15)	
Cu(2)–P(2)	–	2.243(8)	C(55)–C(56)	1.417(15)	
			C(56)–C(57)	1.409(15)	

Å). Each ruthenium atom is ligated by three terminal carbonyl ligands and the two hydrido ligands cap adjacent $CuRu_2$ faces (Cu(1)Ru(1)Ru(2) and Cu(1)Ru(1)Ru(3)).

Figure 2 provides a comparison of the metal–metal separations in VIII with those previously reported for the PPh_3-containing cluster I [2] and for $[Cu_2Ru_4(\mu_3\text{-}H)_2\{\mu\text{-}Ph_2P(CH_2)_2PPh_2\}(CO)_{12}]$ [10]. The latter species, in which the Cu–Cu vector is bridged by a bidentate ligand with a backbone of roughly comparable length to that of the $P(CH_2Ph)_3$ ligand in VIII, exhibits a similar capped trigonal bipyramidal skeletal geometry to those adopted by I and VIII and it crystallizes with two independent molecules in the asymmetric unit. Data for both of these molecules are presented in Figure 2. As expected, the Cu–Cu separation in VIII is ca. 0.17 Å shorter than the length of the unbridged Cu–Cu vector in I. This shortening of the Cu–Cu distance is slightly less that that observed for the $Ph_2P(CH_2)_2PPh_2$-containing species (ca. 0.2 Å). The Cu–Ru distances in VIII show considerable variations, from 2.585(2) Å (Cu(2)–Ru(2)) to 2.813(1) (Cu(1)–Ru(2)). The lengths of the equivalent Cu–Ru vectors in the three clusters also vary considerably in many cases, with the largest difference of ca. 0.14 Å being observed for Cu(1)–Ru(2) in VIII and the corresponding separation in the PPh_3-containing species I (Fig. 2). These significant variations in Cu–Ru distances are not surprising, as the relative "softness" of the metal–metal bonding in Group IB metal heteronuclear clusters is well-established [1,11–13].

Clearly, in the formation of VIII, the steric problems which would arise if bulky $P(CH_2Ph)_3$ groups were attached to two adjacent copper atoms are avoided by one $P(CH_2Ph)_3$ ligand adopting a novel bidentate bonding mode, rather than by an alteration in metal framework geometry, as previously observed [6] for the PCy_3-containing species III. To the best of our knowledge, there is no previous example of an organophosphine ligand bridging two metal atoms in a transition metal cluster compound via bonds from the phosphorus atom and an η^2-CH_2Ph ring. However, η^2-bonding of toluene ligands to copper atoms has been reported [14] for the octanuclear cluster compound $[Cu_2Ru_6(CO)_{18}(C_6H_5Me)_2]$.

Having established the solid-state structure of VIII, the variable-temperature ^1H and $^{31}P\text{-}\{^1H\}$ NMR spectra (Table 2) of this cluster can be interpreted in detail. At ambient temperature, the $^{31}P\text{-}\{^1H\}$ NMR spectrum of VIII consists of a singlet, broadened by quadrupolar effects [2,10,15–17]. A singlet is also observed in the $^{31}P\text{-}\{^1H\}$ NMR spectrum of VIII at $-100\,^\circ C$. This spectrum is in marked contrast to the low temperature $^{31}P\text{-}\{^1H\}$ NMR spectra of the closely related species $[Cu_2Ru_4(\mu_3\text{-}H)_2\{\mu\text{-}Ph_2As(CH_2)_nPPh_2\}(CO)_{12}]$ ($n = 1$ or 2) [18], in which two signals, corresponding to the two different structural isomers * of these clusters, are observed. Thus, although it is possible, in principle, for VIII to exhibit similar structural isomerism to that observed for the $Ph_2As(CH_2)_nPPh_2$-containing clusters, there is no evidence for the presence of a second isomer of VIII in solution at low temperatures. At ambient temperature, the high field hydrido ligand signal in the ^1H NMR spectrum of VIII is a doublet (J(PH) 12Hz). The value of J(PH) for VIII is considerably higher than those of 5–7 Hz observed at ambient temperature

* The two different structural isomers exist for both clusters, because an arsenic atom or a phosphorus atom can be attached to each of the two distinct copper sites in the capped trigonal bipyramidal metal frameworks of these species.

Table 4. Selected bond angles (°), with estimated standard deviations in parentheses, for $[Cu_2Ru_4(\mu_3\text{-}H)_2(CO)_{12}\{\mu\text{-}P(CH_2Ph)_2(\eta^2\text{-}CH_2Ph)\}]$ (VIII) and $[Cu_2Ru_4(\mu_3\text{-}H)_2(CO)_{12}\{P(CH_2Ph)_3\}_2]$ (IX)

(a) VIII			
Ru(3)–Ru(1)–Ru(2)	58.8(1)	Ru(4)–Ru(1)–Ru(2)	58.4(1)
Ru(4)–Ru(1)–Ru(3)	57.6(1)	Cu(1)–Ru(1)–Ru(2)	59.6(1)
Cu(1)–Ru(1)–Ru(3)	56.9(1)	Cu(1)–Ru(1)–Ru(4)	105.2(1)
C(11)–Ru(1)–Ru(2)	125.7(3)	C(11)–Ru(1)–Ru(3)	118.5(3)
C(11)–Ru(1)–Ru(4)	173.0(3)	C(11)–Ru(1)–Cu(1)	74.8(3)
C(12)–Ru(1)–Ru(2)	134.0(3)	C(12)–Ru(1)–Ru(3)	93.7(4)
C(12)–Ru(1)–Ru(4)	75.9(3)	C(12)–Ru(1)–Cu(1)	137.7(4)
C(12)–Ru(1)–C(11)	99.3(4)	C(13)–Ru(1)–Ru(2)	94.5(3)
C(13)–Ru(1)–Ru(3)	146.8(3)	C(13)–Ru(1)–Ru(4)	92.6(3)
C(13)–Ru(1)–Cu(1)	129.4(3)	C(13)–Ru(1)–C(11)	92.6(4)
C(13)–Ru(1)–C(12)	92.3(5)	Ru(3)–Ru(2)–Ru(1)	61.2(1)
Ru(4)–Ru(2)–Ru(1)	58.4(1)	Ru(4)–Ru(2)–Ru(3)	58.4(1)
Cu(1)–Ru(2)–Ru(1)	56.0(1)	Cu(1)–Ru(2)–Ru(3)	56.6(1)
Cu(1)–Ru(2)–Ru(4)	102.3(1)	Cu(2)–Ru(2)–Ru(1)	105.0(1)
Cu(2)–Ru(2)–Ru(3)	58.0(1)	Cu(2)–Ru(2)–Ru(4)	113.0(1)
Cu(2)–Ru(2)–Cu(1)	55.7(1)	C(21)–Ru(2)–Ru(1)	147.3(3)
C(21)–Ru(2)–Ru(3)	95.0(4)	C(21)–Ru(2)–Ru(4)	90.6(3)
C(21)–Ru(2)–Cu(1)	131.4(4)	C(21)–Ru(2)–Cu(2)	76.0(4)
C(22)–Ru(2)–Ru(1)	118.5(3)	C(22)–Ru(2)–Ru(3)	126.0(3)
C(22)–Ru(2)–Ru(4)	173.7(3)	C(22)–Ru(2)–Cu(1)	78.6(3)
C(22)–Ru(2)–Cu(2)	72.8(3)	C(22)–Ru(2)–C(21)	93.4(4)
C(23)–Ru(2)–Ru(1)	89.6(3)	C(23)–Ru(2)–Ru(3)	135.8(3)
C(23)–Ru(2)–Ru(4)	78.4(2)	C(23)–Ru(2)–Cu(1)	134.0(3)
C(23)–Ru(2)–Cu(2)	164.7(3)	C(23)–Ru(2)–C(21)	94.3(5)
C(23)–Ru(2)–C(22)	96.4(4)	Ru(2)–Ru(3)–Ru(1)	59.9(1)
Ru(4)–Ru(3)–Ru(1)	58.1(1)	Ru(4)–Ru(3)–Ru(2)	58.9(1)
Cu(1)–Ru(3)–Ru(1)	56.4(1)	Cu(1)–Ru(3)–Ru(2)	59.9(1)
Cu(1)–Ru(3)–Ru(4)	105.3(1)	Cu(2)–Ru(3)–Ru(1)	101.6(1)
Cu(2)–Ru(3)–Ru(2)	54.9(1)	Cu(2)–Ru(3)–Ru(4)	110.6(1)
Cu(2)–Ru(3)–Cu(1)	55.9(1)	C(31)–Ru(3)–Ru(1)	122.5(3)
C(31)–Ru(3)–Ru(2)	119.7(3)	C(31)–Ru(3)–Ru(4)	178.3(3)
C(31)–Ru(3)–Cu(1)	74.4(3)	C(31)–Ru(3)–Cu(2)	67.8(3)
C(32)–Ru(3)–Ru(1)	137.2(4)	C(32)–Ru(3)–Ru(2)	90.6(3)
C(32)–Ru(3)–Ru(4)	80.7(3)	C(32)–Ru(3)–Cu(1)	136.5(3)
C(32)–Ru(3)–Cu(2)	81.3(3)	C(32)–Ru(3)–C(31)	98.4(5)
C(33)–Ru(3)–Ru(1)	95.6(4)	C(33)–Ru(3)–Ru(2)	147.5(4)
C(33)–Ru(3)–Ru(4)	90.7(3)	C(33)–Ru(3)–Cu(1)	126.6(3)
C(33)–Ru(3)–Cu(2)	157.6(4)	C(33)–Ru(3)–C(31)	90.9(4)
C(33)–Ru(3)–C(32)	95.8(4)	Ru(2)–Ru(4)–Ru(1)	63.3(1)
Ru(3)–Ru(4)–Ru(1)	64.4(1)	Ru(3)–Ru(4)–Ru(2)	62.7(1)
C(41)–Ru(4)–Ru(1)	105.7(3)	C(41)–Ru(4)–Ru(2)	156.5(4)
C(41)–Ru(4)–Ru(3)	94.0(4)	C(42)–Ru(4)–Ru(1)	97.3(3)
C(42)–Ru(4)–Ru(2)	107.7(3)	C(42)–Ru(4)–Ru(3)	161.4(3)
C(42)–Ru(4)–C(41)	93.8(5)	C(43)–Ru(4)–Ru(1)	159.1(3)
C(43)–Ru(4)–Ru(2)	96.3(3)	C(43)–Ru(4)–Ru(3)	103.8(4)
C(43)–Ru(4)–C(41)	91.8(5)	C(43)–Ru(4)–C(42)	92.7(5)
Ru(2)–Cu(1)–Ru(1)	64.4(1)	Ru(3)–Cu(1)–Ru(1)	66.7(1)
Ru(3)–Cu(1)–Ru(2)	63.5(1)	Cu(2)–Cu(1)–Ru(1)	114.0(1)
Cu(2)–Cu(1)–Ru(2)	57.6(1)	Cu(2)–Cu(1)–Ru(3)	61.3(1)
P–Cu(1)–Ru(1)	145.9(1)	P–Cu(1)–Ru(2)	141.7(1)
P–Cu(1)–Ru(3)	137.0(1)	P–Cu(1)–Cu(2)	100.1(1)
Ru(3)–Cu(2)–Ru(2)	67.1(1)	Cu(1)–Cu(2)–Ru(2)	66.7(1)
Cu(1)–Cu(2)–Ru(3)	62.8(1)	C(56)–Cu(2)–Ru(2)	136.6(3)
C(56)–Cu(2)–Ru(3)	143.3(3)	C(56)–Cu(2)–Cu(1)	144.1(2)
C(57)–Cu(2)–Ru(2)	160.8(3)	C(57)–Cu(2)–Ru(3)	130.3(3)
C(57)–Cu(2)–Cu(1)	111.2(3)	C(57)–Cu(2)–C(56)	36.3(4)
Ru–C–O	169.1(7)–179.0(9)		

Table 4 (continued)

(b) IX			
Ru(3)–Ru(1)–Ru(2)	56.7(1)	Ru(4)–Ru(1)–Ru(2)	57.1(1)
Ru(4)–Ru(1)–Ru(3)	59.2(1)	Cu(1)–Ru(1)–Ru(2)	56.3(1)
Cu(1)–Ru(1)–Ru(3)	56.3(1)	Cu(1)–Ru(1)–Ru(4)	104.1(1)
C(11)–Ru(1)–Ru(2)	121(1)	C(11)–Ru(1)–Ru(3)	120(1)
C(11)–Ru(1)–Ru(4)	178(1)	C(11)–Ru(1)–Cu(1)	74(1)
C(12)–Ru(1)–Ru(2)	146(1)	C(12)–Ru(1)–Ru(3)	103(1)
C(12)–Ru(1)–Ru(4)	89(1)	C(12)–Ru(1)–Cu(1)	139.4(9)
C(12)–Ru(1)–C(11)	92(2)	C(13)–Ru(1)–Ru(2)	90.8(8)
C(13)–Ru(1)–Ru(3)	139(1)	C(13)–Ru(1)–Ru(4)	83(1)
C(13)–Ru(1)–Cu(1)	128.1(9)	C(13)–Ru(1)–C(11)	97(2)
C(13)–Ru(1)–C(12)	91(1)	Ru(3)–Ru(2)–Ru(1)	61.9(1)
Ru(4)–Ru(2)–Ru(1)	58.4(1)	Ru(4)–Ru(2)–Ru(3)	61.6(1)
Cu(1)–Ru(2)–Ru(1)	57.3(1)	Cu(1)–Ru(2)–Ru(3)	58.6(1)
Cu(1)–Ru(2)–Ru(4)	105.9(1)	C(21)–Ru(2)–Ru(1)	103.3(9)
C(21)–Ru(2)–Ru(3)	162.3(8)	C(21)–Ru(2)–Ru(4)	103.0(9)
C(21)–Ru(2)–Cu(1)	124(1)	C(22)–Ru(2)–Ru(1)	122.0(9)
C(22)–Ru(2)–Ru(3)	101.0(9)	C(22)–Ru(2)–Ru(4)	161(1)
C(22)–Ru(2)–Cu(1)	66.6(8)	C(22)–Ru(2)–C(21)	95(1)
C(23)–Ru(2)–Ru(1)	136.9(9)	C(23)–Ru(2)–Ru(3)	90.3(9)
C(23)–Ru(2)–Ru(4)	79.9(9)	C(23)–Ru(2)–Cu(1)	136.3(9)
C(23)–Ru(2)–C(21)	96(1)	C(23)–Ru(2)–C(22)	94(1)
Ru(2)–Ru(3)–Ru(1)	61.4(1)	Ru(4)–Ru(3)–Ru(1)	57.2(1)
Ru(4)–Ru(3)–Ru(2)	58.0(1)	Cu(1)–Ru(3)–Ru(1)	57.0(1)
Cu(1)–Ru(3)–Ru(2)	58.3(1)	Cu(1)–Ru(3)–Ru(4)	103.0(1)
Cu(2)–Ru(3)–Ru(1)	77.3(1)	Cu(2)–Ru(3)–Ru(2)	114.3(1)
Cu(2)–Ru(3)–Ru(4)	56.8(1)	Cu(2)–Ru(3)–Cu(1)	131.8(2)
C(31)–Ru(3)–Ru(1)	117(1)	C(31)–Ru(3)–Ru(2)	91.6(9)
C(31)–Ru(3)–Ru(4)	148.9(8)	C(31)–Ru(3)–Cu(1)	60(1)
C(31)–Ru(3)–Cu(2)	154.1(9)	C(32)–Ru(3)–Ru(1)	140(1)
C(32)–Ru(3)–Ru(2)	90(1)	C(32)–Ru(3)–Ru(4)	84(1)
C(32)–Ru(3)–Cu(1)	133(1)	C(32)–Ru(3)–Cu(2)	91(1)
C(32)–Ru(3)–C(31)	90(1)	C(33)–Ru(3)–Ru(1)	112.8(9)
C(33)–Ru(3)–Ru(2)	174(1)	C(33)–Ru(3)–Ru(4)	120.3(8)
C(33)–Ru(3)–Cu(1)	119(1)	C(33)–Ru(3)–Cu(2)	63.5(8)
C(33)–Ru(3)–C(31)	91(1)	C(33)–Ru(3)–C(32)	95(1)
Ru(2)–Ru(4)–Ru(1)	64.6(1)	Ru(3)–Ru(4)–Ru(1)	63.6(1)
Ru(3)–Ru(4)–Ru(2)	60.3(1)	Cu(2)–Ru(4)–Ru(1)	80.5(1)
Cu(2)–Ru(4)–Ru(2)	116.0(1)	Cu(2)–Ru(4)–Ru(3)	56.3(1)
C(41)–Ru(4)–Ru(1)	95(1)	C(41)–Ru(4)–Ru(2)	158(1)
C(41)–Ru(4)–Ru(3)	120.5(9)	C(41)–Ru(4)–Cu(2)	66(1)
C(42)–Ru(4)–Ru(1)	104(1)	C(42)–Ru(4)–Ru(2)	85(1)
C(42)–Ru(4)–Ru(3)	145(1)	C(42)–Ru(4)–Cu(2)	157.6(9)
C(42)–Ru(4)–C(41)	92(1)	C(43)–Ru(4)–Ru(1)	164(1)
C(43)–Ru(4)–Ru(2)	107.9(9)	C(43)–Ru(4)–Ru(3)	100(1)
C(43)–Ru(4)–Cu(2)	91(1)	C(43)–Ru(4)–C(41)	94(1)
C(43)–Ru(4)–C(42)	89(2)	Ru(2)–Cu(1)–Ru(1)	66.4(1)
Ru(3)–Cu(1)–Ru(1)	66.7(1)	Ru(3)–Cu(1)–Ru(2)	63.1(1)
P(1)–Cu(1)–Ru(1)	137.9(3)	P(1)–Cu(1)–Ru(2)	138.3(2)
P(1)–Cu(1)–Ru(3)	147.6(3)	C(31)–Cu(1)–Ru(1)	109.5(7)
C(31)–Cu(1)–Ru(2)	84.7(6)	C(31)–Cu(1)–Ru(3)	43.1(6)
C(31)–Cu(1)–P(1)	106.8(7)	Ru(4)–Cu(2)–Ru(3)	66.9(1)
P(2)–Cu(2)–Ru(3)	149.8(3)	P(2)–Cu(2)–Ru(4)	142.7(2)
C(33)–Cu(2)–Ru(3)	43.7(7)	C(33)–Cu(2)–Ru(4)	110.6(7)
C(33)–Cu(2)–P(2)	106.3(7)	C(41)–Cu(2)–Ru(3)	108.9(7)
C(41)–Cu(2)–Ru(4)	43.4(7)	C(41)–Cu(2)–P(2)	101.2(8)
C(41)–Cu(2)–C(33)	152(1)	C(51)–P(1)–Cu(1)	112(1)
Ru–C–O	167(2)–176(3)		

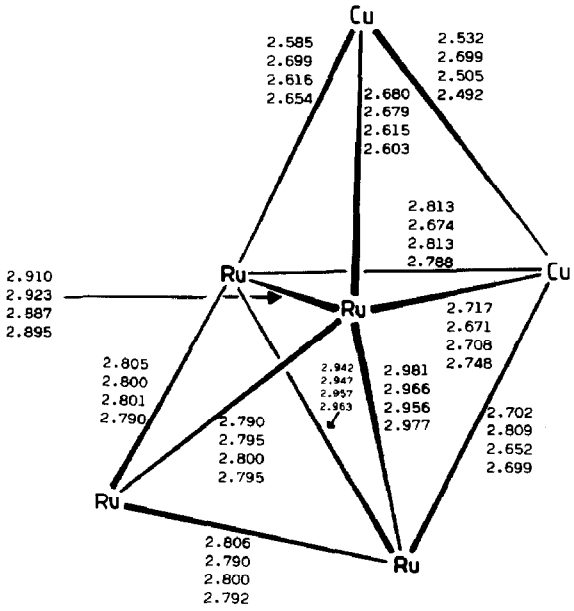

Fig. 2. A comparison of the metal–metal separations (Å) within the capped trigonal bipyramidal metal cores of $[Cu_2Ru_4(\mu_3\text{-}H)_2(CO)_{12}\{\mu\text{-}P(CH_2Ph)_2(\eta^2\text{-}CH_2Ph)\}]$ (VIII), $[Cu_2Ru_4(\mu_3\text{-}H)_2(CO)_{12}(PPh_3)_2]$ (I), and the two independent molecules in the asymmetric unit of $[Cu_2Ru_4(\mu_3\text{-}H)_2\{\mu\text{-}Ph_2P(CH_2)_2PPh_2\}(CO)_{12}]$. Distances are given in the following descending order: VIII, I [2], molecule A of $[Cu_2Ru_4(\mu_3\text{-}H)_2\{\mu\text{-}Ph_2P(CH_2)_2PPh_2\}(CO)_{12}]$ [10], molecule B of $[Cu_2Ru_4(\mu_3\text{-}H)_2\{\mu\text{-}Ph_2P(CH_2)_2PPh_2\}(CO)_{12}]$ [10].

[2,3,10] for I, the phosphine-containing members of the series of clusters II, and $[Cu_2Ru_4(\mu_3\text{-}H)_2\{\mu\text{-}Ph_2P(CH_2)_nPPh_2\}(CO)_{12}]$ ($n = 1$–6), which all undergo intramolecular core rearrangements in solution at this temperature. Interestingly, at low temperatures, spectra consistent with the capped trigonal bipyramidal ground state structures of I, the phosphine-containing members of the series of clusters II, and $[Cu_2Ru_4(\mu_3\text{-}H)_2\{\mu\text{-}Ph_2E(CH_2)_nPPh_2\}(CO)_{12}]$ (E = P, $n = 1$–6; E = As, $n = 1$ or 2) were obtained and, significantly, the magnitude of J(PH) is in the range 12–14 Hz [2,3,10,18], similar to that for VIII at ambient temperature. Thus, the ^{1}H NMR data show that the metal framework of VIII is stereochemically rigid in solution at ambient temperature, which is in marked contrast to the behaviour of the clusters $[Cu_2Ru_4(\mu_3\text{-}H)_2\{\mu\text{-}Ph_2E(CH_2)_nPPh_2\}(CO)_{12}]$ (E = P, $n = 1$–6; E = As, $n = 1$ or 2), in which a coinage metal site-exchange process still occurs even though the copper atoms are bridged by the bidentate ligands [10,18].

The variable-temperature ^{1}H NMR spectroscopic study also shows that the $P(CH_2Ph)_3$ ligand is involved in two intramolecular fluxional processes. At $-100\,^\circ$C, two sets of signals (in the ratio 2/1), corresponding to the two distinct types of CH_2Ph ring in the ground state structure of VIII (Fig. 1), are observed in the ^{1}H NMR spectrum. However, at ambient temperature, only one set of signals due to CH_2Ph groups is present in the ^{1}H NMR spectrum of VIII. Clearly, at ambient temperature in solution, VIII undergoes a novel fluxional process that involves intramolecular exchange of the three CH_2Ph rings between the site in which they are coordinated to the copper atom and the two uncoordinated positions. Despite the fact that dynamic behaviour involving intermolecular exchange of

PR_3 (R = alkyl or aryl) ligands between clusters has been previously reported for some copper-containing heteronuclear clusters [17,19], this process can be ruled out as a possible explanation for the variable-temperature NMR spectra of VIII, because $^{31}P-^{1}H$ coupling is still observed between the $P(CH_2Ph)_3$ group and the hydrido ligands at ambient temperature. In addition, although there is a plane of symmetry through Cu(1), Cu(2), Ru(1), and Ru(4) (Fig. 1) in the metal skeleton of VIII, the conformation adopted by the CH_2Ph ring, which is coordinated to Cu(2) in the ground state structure of the cluster, renders the two hydrido ligands H(1) and H(2) inequivalent. Interestingly, however, only a single high field hydrido ligand resonance is observed in the ^{1}H NMR spectrum of VIII at $-100\,^{\circ}C$, which is a temperature low enough to prevent occurrence of the CH_2Ph ring site-exchange process described above. Thus, at $-100\,^{\circ}C$, VIII must undergo an additional dynamic process, which renders the two hydrido ligands equivalent, and there are two possible explanations for the observed results. The two hydrido ligands themselves may be undergoing dynamic behaviour involving site-exchange or the CH_2Ph ring, which is coordinated to Cu(2), may be undergoing rapid exchange between the various possible conformations. A rapid exchange of the methylene groups in the backbones of the bidentate ligands between the various possible conformations has been recently suggested [16] as a more reasonable explanation for the observed equivalence of the hydrido ligands in the series of clusters $[Cu_2Ru_4(\mu_3\text{-}H)_2\{\mu\text{-}Ph_2E(CH_2)_nPPh_2\}(CO)_{12}]$ (E = P, $n = 1$–6; E = As, $n = 1$ or 2) than a hydrido ligand site-exchange process for two reasons. Firstly, the free energy of activation for the process was found to be altered very considerably by changes in the number of methylene groups in the backbones of the bidentate ligands and by the formal replacement of phosphorus by arsenic. Secondly, a hydrido ligand site-exchange process could not account for the band-shape changes and/or broadening, which were observed for the methylene group signals in the ^{1}H NMR spectra of some of the above clusters on cooling. Therefore, although dynamic behaviour involving hydrido ligand site-exchange is well-established for transition metal cluster compounds [2,11,20], because of the close similarity between VIII and $[Cu_2Ru_4(\mu_3\text{-}H)_2\{\mu\text{-}Ph_2E(CH_2)_nPPh_2\}(CO)_{12}]$ (E = P, $n = 1$–6; E = As, $n = 1$ or 2), we propose that the observed equivalence of the hydrido ligands in VIII is caused by a dynamic process, which involves the coordinated CH_2Ph ring undergoing rapid exchange between the various possible conformations.

In an attempt to synthesize a hexanuclear cluster compound of formula $[Cu_2Ru_4(\mu_3\text{-}H)_2(CO)_{12}\{P(CH_2Ph)_3\}_2]$, we treated an acetone solution of the salt $[N(PPh_3)_2]_2[Ru_4(\mu\text{-}H)_2(CO)_{12}]$ with a dichloromethane solution containing two equivalents of the complex $[CuCl\{P(CH_2Ph)_3\}]$, in the presence of $TlPF_6$. This reaction afforded a mixture of the previously characterized species $[Cu_2Ru_4(\mu_3\text{-}H)_2(CO)_{12}\{\mu\text{-}P(CH_2Ph)_2(\eta^2\text{-}CH_2Ph)\}]$ (VIII) (44% yield) and the new compound $[Cu_2Ru_4(\mu_3\text{-}H)_2(CO)_{12}\{P(CH_2Ph)_3\}_2]$ (IX) (12% yield). The clusters VIII and IX were readily separated and purified by column chromatography on Florisil at $-20\,^{\circ}C$. The analytical and spectroscopic data of the samples of VIII, which were prepared by the two alternative routes, are identical and the new species IX was characterized by microanalysis and spectroscopic measurements (Tables 1 and 2). The IR and NMR spectra of IX are significantly different from those reported [2,3] for the series of clusters I and II, which exhibit capped trigonal bipyramidal skeletal geometries with the two copper atoms in close contact, but they are closely similar

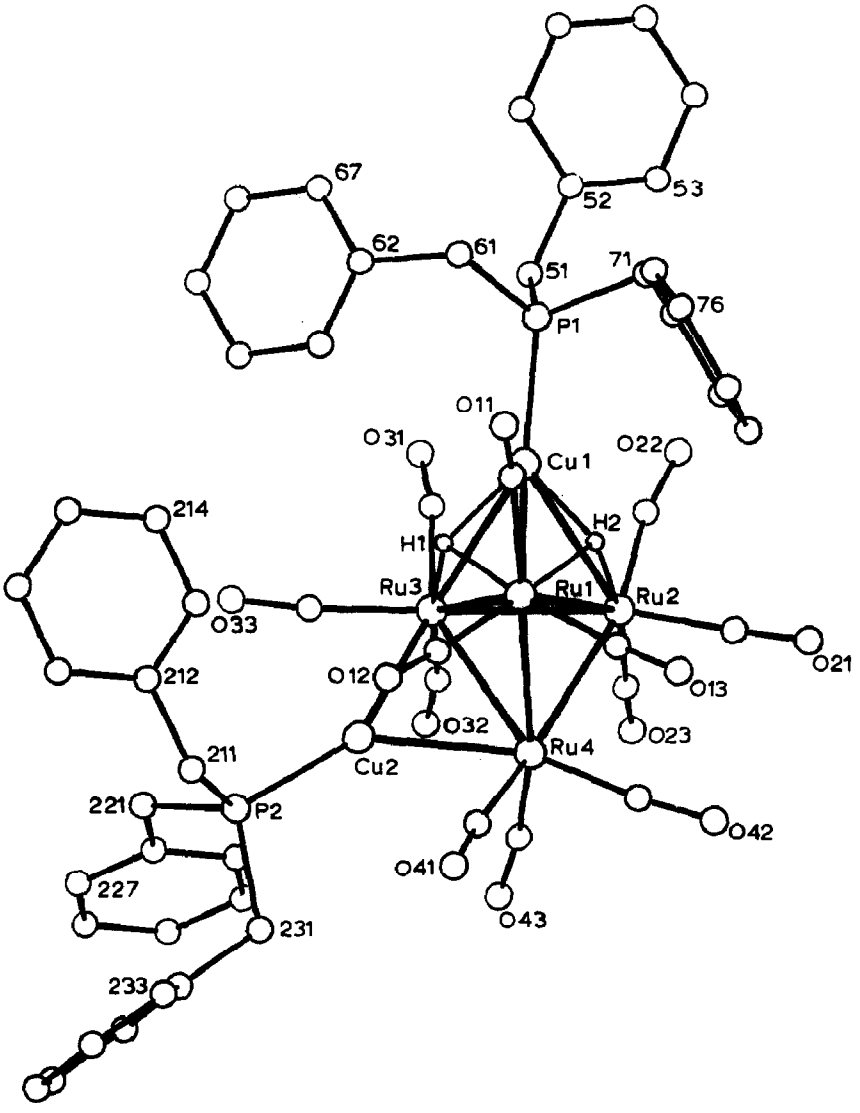

Fig. 3. Molecular structure of $[Cu_2Ru_4(\mu_3\text{-}H)_2(CO)_{12}\{P(CH_2Ph)_3\}_2]$ (IX), showing the crystallographic numbering. The carbon atom of each carbonyl group has the same number as the oxygen atom.

to those of the PCy_3-ligated species III [6]. Thus, it seemed very likely that IX adopts a similar sterically less demanding metal framework structure, consisting of a Ru_4 tetrahedron with one edge bridged by a $Cu\{P(CH_2Ph)_3\}$ unit and a non-adjacent face capped by the second $Cu\{P(CH_2Ph)_3\}$ group, to that previously established [6] for III and this has been confirmed by a single-crystal X-ray diffraction study.

The molecular structure of IX is shown in Fig. 3 and selected interatomic distances and angles are presented in Tables 3 and 4, respectively. The metal framework of IX consists of a Ru_4 tetrahedron, with one Ru_3 face (Ru(1)Ru(2)Ru(3)) capped by a copper atom (Cu(1)) and one Ru–Ru edge (Ru(3)–Ru(4)) bridged by the second copper atom (Cu(2)). In marked contrast to the structure of VIII, both copper atoms in IX are ligated by $P(CH_2Ph)_3$ groups and these ligands are bonded

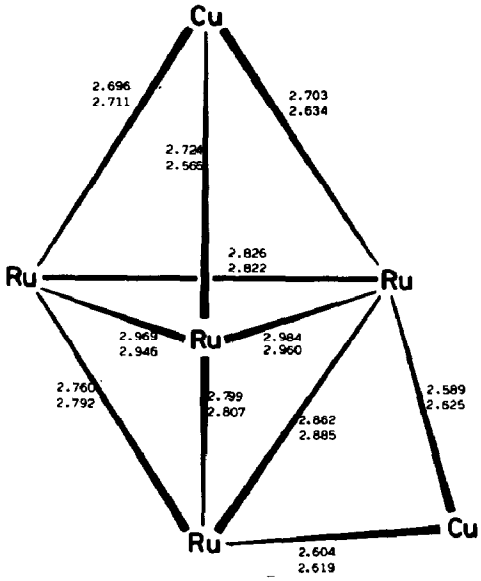

Fig. 4. A comparison of the metal–metal separations (Å) within the edge-bridged trigonal bipyramidal metal cores of $[Cu_2Ru_4(\mu_3\text{-}H)_2(CO)_{12}(PR_3)_2]$ (R = CH_2Ph (IX) or Cy (III)). Distances are given first for IX, then for III [6].

via their phosphorus atoms only. Three terminal carbonyl groups are bonded to each ruthenium atom and the two hydrido ligands cap adjacent $CuRu_2$ faces (Cu(1)Ru(1)Ru(2) and Cu(1)Ru(1)Ru(3)).

Figure 4 compares the metal–metal separations in IX with those of the PCy_3-ligated species III, which is the only previously reported [6] cluster with a similar skeletal geometry. As expected [1,11–13], the lengths of the equivalent Cu–Ru vectors in IX and III vary considerably in many cases, with the largest difference of ca. 0.16 Å being observed for Cu(1)–Ru(1). In addition, there are some very short contact distances between the carbonyl carbon atoms and the copper atoms in IX (Cu(1)...C(31) 2.42(4), Cu(2)...C(33) 2.43(3), and Cu(2)...C(41) 2.52(3) Å). Similar structural features have been previously observed for a considerable number of Group IB metal heteronuclear cluster compounds, but the exact nature of the interaction is not well-understood [12].

The skeletal geometry of IX is very unusual. In almost all previously reported mixed-metal clusters containing two or more $M(PR_3)$ (M = Cu, Ag, or Au; R = alkyl or aryl) units, the Group IB metal fragments either all adopt face-capping positions or all occupy edge-bridging sites [12]. Also, whenever there is a possibility that a $Cu(PR_3)$ group can adopt either an edge-bridging or a face-capping position, the latter bonding mode is preferred in almost every case [12]. Presumably, it is the size of the phosphine ligands in IX and in III that forces one of the $Cu(PR_3)$ (R = CH_2Ph or Cy) fragments to adopt an apparently less favourable, but also sterically less demanding, bonding mode.

Interestingly, although there are two distinct phosphorus environments in the structure of IX in the solid state, the ambient temperature $^{31}P\text{-}\{^1H\}$ NMR spectrum of the cluster is a singlet, broadened by quadrupolar effects [2,10,15–17] (Table 2). However, at −100 °C, two broad singlets are observed, which is consistent with the ground state structure of IX (Fig. 3). Clearly, at ambient temperature in solution, IX

undergoes some form of dynamic behaviour that renders the two phosphorus environments equivalent and the $^{31}P-^{1}H$ coupling observed for the high field hydrido ligand signal in the ambient temperature ^{1}H NMR spectrum of the cluster demonstrates that this process must be intramolecular. Thus, the two $Cu\{P(CH_2Ph)_3\}$ units in IX must be interchanging between edge-bridging and face-capping bonding modes at ambient temperature in solution and this dynamic process must also be accompanied by a concomitant site-exchange process for the two hydrido ligands. The proposed hydrido ligand site-exchange process is consistent with the variable-temperature ^{1}H NMR spectra observed for IX (Table 2). At $-100\,^{\circ}C$, two high field hydrido ligand doublets (J(PH) 9 Hz) are present in the ^{1}H NMR spectrum of IX, which is consistent with the two distinct hydrido ligand environments in the solid state structure (Fig. 3), whereas a single hydrido ligand resonance (broad triplet, J(PH) 5 Hz) is observed at ambient temperature. Interestingly, similar dynamic behaviour, which involves the interchange of $Cu(PCy_3)$ fragments between edge-bridging and face-capping bonding modes, together with a concomitant hydrido ligand site-exchange process, has been previously reported [6] for the closely related PCy_3-ligated species III. The interchange of the $Cu(PR_3)$ ($R = CH_2Ph$ or Cy) groups between the two different bonding modes that is observed for III and IX is particularly interesting in view of the theoretical work of Mingos [21], which suggests that such a process should be facile.

The structure adopted by IX clearly demonstrates that the $P(CH_2Ph)_3$ ligand is too bulky to allow two $Cu\{P(CH_2Ph)_3\}$ units to be adjacent in the metal skeleton of the cluster. However, it is very interesting that both VIII and IX, which exhibit such distinctly different ways of solving the problem of accommodating the sterically demanding $P(CH_2Ph)_3$ ligand in their metal framework structures, can actually be isolated from the same reaction.

In marked contrast to the previously described preparation of the copper-containing cluster VIII, treatment of a dichloromethane solution of the salt $[N(PPh_3)_2]_2[Ru_4(\mu\text{-}H)_2(CO)_{12}]$ with two equivalents of the complex $[Ag(NCMe)_4]PF_6$ at $-30\,^{\circ}C$, followed by the addition of two equivalents of $P(CH_2Ph)_3$, affords the expected [2–5] mixed-metal cluster compound $[Ag_2Ru_4(\mu_3\text{-}H)_2(CO)_{12}\{P(CH_2Ph)_3\}_2]$ (X) (37% yield). The IR and low temperature NMR spectroscopic data (Tables 1 and 2) of X are very similar to those previously reported [2,4,5] for the series of silver-containing clusters V–VII. At $-90\,^{\circ}C$, the $^{31}P\text{-}\{^{1}H\}$ NMR spectrum of X consists of two resonances, each of which is split into two doublets by large $^{107}Ag-^{31}P$ and $^{109}Ag-^{31}P$ couplings through one bond. These doublets are all further split by much smaller $^{107,109}Ag-^{31}P$ couplings through two bonds. The magnitudes of these latter couplings are not sufficient to allow resolution of the separate contributions from ^{107}Ag and ^{109}Ag. The high field hydrido ligand signal in the ^{1}H NMR spectrum of X at $-80\,^{\circ}C$ is split into a doublet of doublets by couplings to one silver atom and one phosphorus atom ($J(AgH)_{av.}$ 25, J(PH) 8 Hz). The spectroscopic data observed for X demonstrate that, like those of the analogous PPh_3-containing species V [2], the series of clusters VI, and the PCy_3-ligated compound VII [4,5], the metal framework of X exhibits a capped trigonal bipyramidal skeletal geometry, with the two silver atoms in close contact. Thus, the greater size of the silver atom relative to copper means that X can adopt a metal core structure in which two adjacent $Ag\{P(CH_2Ph)_3\}$ units are accommodated, whereas the bulky $P(CH_2Ph)_3$ ligand forces the analogous copper-containing species IX to adopt a

sterically less demanding skeletal geometry. The metal framework structure established for X is not surprising in view of the fact that the PCy_3-ligated species VII is known [5] to adopt a similar skeletal geometry, with two adjacent $Ag(PCy_3)$ groups, and the cone angle of PCy_3 is 5° larger than that of $P(CH_2Ph)_3$ [7].

As the temperature is raised from −90 °C, the two phosphorus resonances in the $^{31}P-\{^1H\}$ NMR spectrum of X coalesce. At ambient temperature a complex multiplet with reasonably narrow linewidths is observed, and this resonance then begins to broaden again as the temperature is increased further. The complex multiplet has a very similar pattern of signals to those previously observed [22] in the ambient temperature $^{31}P-\{^1H\}$ NMR spectra of $[Ag_2Ru_4(\mu_3\text{-}H)_2\{\mu\text{-}Ph_2P(CH_2)_nPPh_2\}(CO)_{12}]$ ($n = 4$ or 5), although not all of the peaks that are observed for the latter two clusters can be fully resolved for X, because the linewidths of the signals for X are not narrow enough at any temperature. Analysis of the signals observed for the two $Ph_2P(CH_2)_nPPh_2$-containing species has shown that they consist of three superimposed sub-spectra due to the $^{107}Ag^{107}Ag$, $^{107}Ag^{109}Ag$, and $^{109}Ag^{109}Ag$ isotopomers of each cluster. In each spectrum, a single phosphorus resonance is split by $^{107,109}Ag-^{31}P$ couplings through one and two bonds and by $^{107,109}Ag-^{107,109}Ag$ couplings and the pattern of signals is further complicated by second order effects [22]. The high field hydrido ligand signal in the ambient temperature ^1H NMR spectrum of X consists of an overlapping triplet of triplets pattern, which is caused by couplings to two equivalent silver atoms and two equivalent phosphorus atoms ($J(AgH)_{av.}$ 12, $J(PH)$ 5 Hz). This signal also broadens as the temperature is raised further. In addition, the CH_2Ph signal in the ^1H NMR spectrum of X at −20 °C, which is split into a doublet of doublets by $^{107,109}Ag-^1H$ and $^{31}P-^1H$ couplings ($J(AgH)_{av.}$ 3, $J(PH)$ 6 Hz), broadens and loses the $^{107,109}Ag-^1H$ coupling as the temperature increases. The variable-temperature NMR data demonstrate that X undergoes two distinct dynamic processes in solution. The coalescence of the two phosphorus resonances in the low temperature $^{31}P-\{^1H\}$ NMR spectra and the observation of equivalent phosphorus atoms in the ambient temperature $^{31}P-\{^1H\}$ and ^1H NMR spectra can be explained in terms of a process involving the two silver atoms in X undergoing intramolecular exchange between the distinct Group IB metal sites in the ground state metal framework structure of the cluster. Similar dynamic behaviour has been previously observed by $^{31}P-\{^1H\}$ and ^1H NMR spectroscopy for the series of analogous clusters V–VII [2,5,23] and also detected directly by $^{109}Ag-\{^1H\}$ INEPT NMR spectroscopy for $[Ag_2Ru_4(\mu_3\text{-}H)_2\{\mu\text{-}Ph_2P(CH_2)_nPPh_2\}(CO)_{12}]$ ($n = 1$, 2, or 4) [22], which all adopt similar capped trigonal bipyramidal metal core structures to that established for X. The free energy of activation ($\Delta G^{\ddagger}$) for the intramolecular metal core rearrangement that X undergoes in solution can be estimated from the coalescence temperature of -30 ± 5 °C observed in the variable-temperature $^{31}P-\{^1H\}$ NMR spectra of the cluster. The $\Delta G^{\ddagger}$ value of 43 ± 1 kJ mol^{-1} calculated for X is ca. 3 kJ mol^{-1} larger than that previously reported [2] for the same dynamic process in the analogous PPh_3-ligated species V. This increase in the magnitude of $\Delta G^{\ddagger}$ as the cone angle of the attached phosphine ligand becomes larger is consistent with the trend in $\Delta G^{\ddagger}$ previously observed [3] for the metal core rearrangements of the closely related copper species I and the phosphine-containing members of the series of clusters II. The loss of $^{107,109}Ag-^1H$ coupling and the other changes in band-shape that are observed in the variable-temperature NMR spectra of X can be accounted for in terms of a process

involving intermolecular exchange of $P(CH_2Ph)_3$ ligands between clusters. Intermolecular exchange of phosphine ligands in solution is well-established for silver-containing heteronuclear clusters [12,17,19] and similar dynamic behaviour has been previously observed [2,5,23] for the series of clusters V–VII, which are analogous to X.

Conclusions

Although a capped trigonal bipyramidal metal core structure, with the Cu atoms in close contact, seems to be the preferred skeletal geometry for clusters of general formula $[Cu_2Ru_4(\mu_3\text{-}H)_2(CO)_{12}L_2]$ when L is a relatively small phosphine or phosphite ligand, when $L = P(CH_2Ph)_3$ the phosphine ligand is too bulky to allow two $Cu\{P(CH_2Ph)_3\}$ units to be adjacent in such a metal framework structure. This problem is solved either by a single $P(CH_2Ph)_3$ ligand bridging both Cu atoms in a novel bidentate bonding mode, as is the case in $[Cu_2Ru_4(\mu_3\text{-}H)_2(CO)_{12}\{\mu\text{-}P(CH_2Ph)_2(\eta^2\text{-}CH_2Ph)\}]$ (VIII), or by the cluster adopting an apparently less favourable skeletal geometry in which only one $Cu\{P(CH_2Ph)_3\}$ group is in a face-capping position and the other occupies a sterically less demanding edge-bridging site, as observed for $[Cu_2Ru_4(\mu_3\text{-}H)_2(CO)_{12}\{P(CH_2Ph)_3\}_2]$ (IX). However, the greater size of the silver atom relative to copper allows two adjacent $Ag\{P(CH_2Ph)_3\}$ groups to be accommodated in the metal skeleton of $[Ag_2Ru_4(\mu_3\text{-}H)_2(CO)_{12}\{P(CH_2Ph)_3\}_2]$ (X) and, therefore, X is able to adopt the preferred capped trigonal bipyramidal metal framework structure, with the two silver atoms in close contact. Variable-temperature $^{31}P\text{-}\{^1H\}$ and ^1H NMR spectroscopic studies demonstrate that each of the clusters VIII–X undergoes a number of interesting dynamic processes in solution.

Experimental

The techniques used and the instrumentation employed have been described elsewhere [18]. Light petroleum refers to the fraction of b.p. 40–60 °C. Established methods were used to prepare the salt $[N(PPh_3)_2]_2[Ru_4(\mu\text{-}H)_2(CO)_{12}]$ [24] and the complex $[Cu(NCMe)_4]PF_6$ [25]. The compound $[Ag(NCMe)_4]PF_6$ was synthesized by an adaptation of a published route [25,26]. The ligand $P(CH_2Ph)_3$ was purchased from Strem Chemicals Inc. and used without further purification. Analytical and physical data for the new Group IB metal heteronuclear cluster compounds are presented in Table 1, together with their IR spectra. Table 2 summarizes the results of NMR spectroscopic measurements. Product separation by column chromatography was performed on Aldrich Florisil (100–200 mesh).

Synthesis of the cluster $[Cu_2Ru_4(\mu_3\text{-}H)_2(CO)_{12}\{\mu\text{-}P(CH_2Ph)_2(\eta^2\text{-}CH_2Ph)\}]$ *(VIII)*

A dichloromethane (40 cm^3) solution of $[N(PPh_3)_2]_2[Ru_4(\mu\text{-}H)_2(CO)_{12}]$ (0.60 g, 0.33 mmol) at −30 °C was treated with a solution of $[Cu(NCMe)_4]PF_6$ (0.25 g, 0.67 mmol) in dichloromethane (25 cm^3). After stirring the reaction mixture at −30 °C for 1 min, a dichloromethane (15 cm^3) solution of $P(CH_2Ph)_3$ (0.10 g, 0.33 mmol) * was added. The mixture was then allowed to warm, with stirring, to ambient

* Essentially the same yield of product is obtained if two equivalents of $P(CH_2Ph)_3$ are used in the reaction instead of one equivalent.

temperature and the solvent was removed under reduced pressure. The crude residue was extracted with a 1/4 dichloromethane/diethyl ether mixture (25 cm^3 portions) until the extracts were no longer red and the combined extracts were filtered through a Celite pad (ca. 1 × 3 cm). After removal of the solvent under reduced pressure, the crude residue was dissolved in a dichloromethane/light petroleum mixture (7/3) and chromatographed at −20 °C on a Florisil column (20 × 3 cm). Elution with a 7/3 dichloromethane/light petroleum mixture gave a single dark red fraction, which, after removal of the solvent under reduced pressure and crystallization of the residue from a dichloromethane/light petroleum mixture, afforded red microcrystals of the copper-ruthenium cluster $[Cu_2Ru_4(\mu_3\text{-}H)_2(CO)_{12}\{\mu\text{-}P(CH_2Ph)_2(\eta^2\text{-}CH_2Ph)\}]$ (VIII) (0.30 g, 77%).

Reaction of $[N(PPh_3)_2]_2[Ru_4(\mu\text{-}H)_2(CO)_{12}]$ with two equivalents of $[CuCl\{P(CH_2Ph)_3\}]$. Synthesis of the clusters $[Cu_2Ru_4(\mu_3\text{-}H)_2(CO)_{12}\{\mu\text{-}P(CH_2Ph)_2(\eta^2\text{-}CH_2Ph)\}]$ (VIII) and $[Cu_2Ru_4(\mu_3\text{-}H)_2(CO)_{12}\{P(CH_2Ph)_3\}_2]$ (IX)

An acetone (40 cm^3) solution of $[N(PPh_3)_2]_2[Ru_4(\mu\text{-}H)_2(CO)_{12}]$ (0.60 g, 0.33 mmol) was treated with a dichloromethane (40 cm^3) solution of $[CuCl\{P(CH_2Ph)_3\}]$ (0.29 g, 0.72 mmol) and solid $TlPF_6$ (0.40 g, 1.15 mmol) and the mixture was stirred at ambient temperature for 1.5 h. After filtration of the dark red solution through a Celite pad (ca. 1 × 3 cm), the solvent was removed under reduced pressure. The residue was then extracted with a 1/4 dichloromethane/diethyl ether mixture (25 cm^3 portions) until the extracts were no longer red and the combined extracts were filtered through a Celite pad (ca. 1 × 3 cm). After removal of the solvent under reduced pressure, the residue was dissolved in a dichloromethane/light petroleum mixture (7/3) and chromatographed at −20 °C on a Florisil column (20 × 3 cm). Elution with a dichloromethane/light petroleum mixture of the same proportions as above gave two red fractions. After removal of the solvent under reduced pressure and crystallization of the residue from a dichloromethane/light petroleum mixture, the first fraction afforded red microcrystals of $[Cu_2Ru_4(\mu_3\text{-}H)_2(CO)_{12}\{P(CH_2Ph)_3\}_2]$ (IX) (0.06 g, 12%) and the second fraction yielded red microcrystals of $[Cu_2Ru_4(\mu_3\text{-}H)_2(CO)_{12}\{\mu\text{-}P(CH_2Ph)_2(\eta^2\text{-}CH_2Ph)\}]$ (VIII) (0.17 g, 44%).

Synthesis of the cluster $[Ag_2Ru_4(\mu_3\text{-}H)_2(CO)_{12}\{P(CH_2Ph)_3\}_2]$ (X)

A dichloromethane (40 cm^3) solution of $[N(PPh_3)_2]_2[Ru_4(\mu\text{-}H)_2(CO)_{12}]$ (0.60 g, 0.33 mmol) at −30 °C was treated with a solution of $[Ag(NCMe)_4]PF_6$ (0.28 g, 0.67 mmol) in dichloromethane (30 cm^3). After stirring the reaction mixture at −30 °C for 1 min, a dichloromethane solution (20 cm^3) of $P(CH_2Ph)_3$ (0.20 g, 0.66 mmol) was added. The mixture was then allowed to warm, with stirring, to ambient temperature and the solvent removed under reduced pressure. The residue was extracted with a 1/4 dichloromethane/diethyl ether mixture (25 cm^3 portions) until the extracts were no longer red and the combined extracts were filtered through a Celite pad (ca. 1 × 3 cm). After removal of the solvent under reduced pressure, the residue was dissolved in a 3/1 dichloromethane/light petroleum mixture and chromatographed at −20 °C on a Florisil column (20 × 3 cm). Elution with a 3/1 dichloromethane/light petroleum mixture gave a single dark red fraction, which after removal of the solvent under reduced pressure and crystallization of the residue from a dichloromethane/light petroleum mixture afforded red microcrystals

Table 5. Fractional atomic coordinates and thermal parameters ($Å^2$) for $[Cu_2Ru_4(\mu_3\text{-}H)_2(CO)_{12}\{\mu\text{-}P(CH_2Ph)_2(\eta^2\text{-}CH_2Ph)\}]$ (VIII), with estimated standard deviations in parentheses.

Atom	x	y	z	U_{iso} or U_{eq}
Ru(1)	0.33332(5)	0.13345(6)	0.11591(6)	0.0332(4)
Ru(2)	0.15618(5)	0.22715(6)	0.08377(6)	0.0320(4)
Ru(3)	0.32882(5)	0.33525(6)	0.02771(6)	0.0328(4)
Ru(4)	0.30357(6)	0.35457(6)	0.26418(6)	0.0371(4)
Cu(1)	0.25437(8)	0.11271(10)	−0.10650(10)	0.0393(6)
Cu(2)	0.16219(9)	0.27669(11)	−0.11198(11)	0.0478(7)
C(11)	0.3680(6)	−0.0096(8)	0.0106(8)	0.042(5)
O(11)	0.3961(6)	−0.0923(7)	−0.0415(7)	0.067(5)
C(12)	0.4509(7)	0.1966(9)	0.2138(10)	0.053(6)
O(12)	0.5212(5)	0.2227(7)	0.2713(7)	0.063(5)
C(13)	0.2902(6)	0.0610(9)	0.2237(9)	0.045(6)
O(13)	0.2655(6)	0.0167(7)	0.2889(7)	0.078(6)
C(21)	0.0949(8)	0.3584(9)	0.1111(10)	0.056(7)
O(21)	0.0528(6)	0.4383(7)	0.1264(9)	0.089(7)
C(22)	0.0549(7)	0.1277(8)	−0.0306(8)	0.041(5)
O(22)	−0.0111(5)	0.0707(7)	−0.0843(6)	0.061(5)
C(23)	0.1168(6)	0.1926(8)	0.2202(9)	0.042(6)
O(23)	0.0889(5)	0.1639(7)	0.2954(6)	0.064(5)
C(31)	0.3422(7)	0.3223(8)	−0.1357(9)	0.042(6)
O(31)	0.3579(5)	0.3324(6)	−0.2265(6)	0.053(4)
C(32)	0.2855(7)	0.4821(9)	0.0769(9)	0.049(6)
O(32)	0.2605(6)	0.5731(7)	0.1010(7)	0.074(6)
C(33)	0.4574(7)	0.3936(9)	0.0746(9)	0.049(6)
O(33)	0.5383(6)	0.4248(8)	0.0933(8)	0.081(6)
C(41)	0.4240(8)	0.4375(10)	0.3277(9)	0.054(7)
O(41)	0.4963(6)	0.4936(8)	0.3695(7)	0.075(6)
C(42)	0.2851(7)	0.3148(9)	0.4033(10)	0.052(6)
O(42)	0.2765(6)	0.2919(7)	0.4878(7)	0.080(6)
C(43)	0.2475(8)	0.4884(10)	0.3186(9)	0.053(7)
O(43)	0.2130(7)	0.5755(7)	0.3539(7)	0.082(6)
P	0.2317(2)	0.0053(2)	−0.2980(2)	0.032(1)
C(51)	0.1821(7)	0.0813(10)	−0.3969(9)	0.046(6)
C(52)	0.103896)	0.1506(8)	−0.3456(8)	0.039(5)
C(53)	0.0148(7)	0.0998(9)	−0.3449(9)	0.043(6)
C(54)	−0.0536(7)	0.1662(10)	−0.2911(10)	0.053(7)
C(55)	−0.0318(7)	0.2864(9)	−0.2318(10)	0.056(7)
C(56)	0.0601(8)	0.3399(9)	−0.2347(9)	0.053(6)
C(57)	0.1273(7)	0.2730(8)	−0.2930(8)	0.041(5)
C(61)	0.3367(6)	−0.0452(8)	−0.3697(8)	0.039(5)
C(62)	0.4151(6)	0.0513(8)	−0.3505(9)	0.042(5)
C(63)	0.4308(7)	0.1052(9)	−0.4360(9)	0.054(6)
C(64)	0.5017(8)	0.1918(10)	−0.4190(11)	0.068(8)
C(65)	0.5651(8)	0.2291(10)	−0.3141(12)	0.069(8)
C(66)	0.5531(8)	0.1792(10)	−0.2287(11)	0.061(7)
C(67)	0.4789(6)	0.0899(8)	−0.2453(9)	0.046(6)
C(71)	0.1491(6)	−0.1316(8)	−0.3380(9)	0.044(6)
C(72)	0.1792(6)	−0.2123(8)	−0.2760(8)	0.040(5)
C(73)	0.1552(8)	−0.2015(10)	−0.1623(11)	0.064(8)
C(74)	0.2604(10)	−0.3760(12)	−0.2692(15)	0.087(10)
C(75)	0.1815(10)	−0.2772(14)	−0.1034(14)	0.096(11)
C(76)	0.2341(11)	−0.3620(14)	−0.1580(15)	0.101(12)
C(77)	0.2324(8)	−0.2980(9)	−0.3272(11)	0.061(7)
H(1)	0.214	0.094	0.032	0.08
H(2)	0.364	0.188	−0.007	0.08
C	0.0085(20)	0.5081(28)	−0.4225(24)	0.093(20)
Cl	0.0447(4)	0.3975(5)	−0.5110(5)	0.156(5)

Table 6

Fractional atomic coordinates and thermal parameters ($Å^2$) for $[Cu_2Ru_4(\mu_3\text{-}H)_2(CO)_{12}\{P(CH_2Ph)_3\}_2]$ (IX), with estimated standard deviations in parentheses

Atom	x	y	z	U_{iso} or U_{eq}
Ru(1)	0.0569(2)	−0.1524(1)	0.3461(2)	0.040(1)
Ru(2)	−0.0947(2)	−0.2534(1)	0.1664(2)	0.039(1)
Ru(3)	0.0955(2)	−0.2803(1)	0.2836(2)	0.042(2)
Ru(4)	0.0688(2)	−0.1581(1)	0.1132(2)	0.042(2)
Cu(1)	−0.0318(3)	−0.2905(2)	0.4098(3)	0.053(2)
Cu(2)	0.2433(2)	−0.1767(2)	0.2486(3)	0.052(2)
P(1)	−0.0973(6)	−0.3495(4)	0.5543(7)	0.054(5)
P(2)	0.4080(5)	−0.1315(4)	0.2794(7)	0.045(5)
C(11)	0.0444(35)	−0.1507(25)	0.5128(46)	0.104(18)
O(11)	0.0520(20)	−0.1433(14)	0.6018(27)	0.104(10)
C(12)	0.1863(24)	−0.0851(16)	0.3866(28)	0.066(10)
O(12)	0.2634(16)	−0.0463(11)	0.4190(19)	0.078(7)
C(13)	−0.0049(22)	−0.0778(16)	0.2667(28)	0.069(9)
O(13)	−0.0468(16)	−0.0328(11)	0.2212(19)	0.083(7)
C(21)	−0.1960(22)	−0.2066(15)	0.0920(27)	0.061(9)
O(21)	−0.2626(17)	−0.1809(12)	0.0415(21)	0.095(8)
C(22)	−0.1769(21)	−0.3370(15)	0.2147(26)	0.058(9)
O(22)	−0.2448(15)	−0.3850(11)	0.2301(19)	0.082(7)
C(23)	−0.1033(21)	−0.2887(15)	0.0240(28)	0.069(9)
O(23)	−0.1159(16)	−0.3137(11)	−0.0609(21)	0.090(7)
C(31)	0.0381(20)	−0.3715(15)	0.3526(25)	0.046(8)
O(31)	0.0132(15)	−0.4313(11)	0.3843(19)	0.070(6)
C(32)	0.0834(23)	−0.3228(17)	0.1480(31)	0.083(10)
O(32)	0.0891(17)	−0.3510(12)	0.0706(22)	0.097(8)
C(33)	0.2245(21)	−0.2906(14)	0.3715(26)	0.045(8)
O(33)	0.2998(17)	−0.3053(11)	0.4285(21)	0.095(8)
C(41)	0.1757(24)	−0.0739(17)	0.1223(29)	0.067(10)
O(41)	0.2346(15)	−0.0190(11)	0.1318(18)	0.076(6)
C(42)	−0.0215(23)	−0.1107(16)	0.0102(29)	0.078(10)
O(42)	−0.0816(16)	−0.0785(11)	−0.0515(20)	0.088(7)
C(43)	0.0806(23)	−0.1868(16)	−0.0213(30)	0.079(10)
O(43)	0.1048(17)	−0.2030(12)	−0.0989(22)	0.093(8)
C(51)	−0.1395(20)	−0.4448(14)	0.5382(26)	0.060(9)
C(52)	−0.2192(17)	−0.4897(10)	0.5947(22)	0.061(9)
C(53)	−0.3211(17)	−0.5053(10)	0.5282(22)	0.117(15)
C(54)	−0.3916(17)	−0.5437(10)	0.5863(22)	0.164(21)
C(55)	−0.3603(17)	−0.5664(10)	0.7109(22)	0.143(17)
C(56)	−0.2585(17)	−0.5507(10)	0.7774(22)	0.120(15)
C(57)	−0.1879(17)	−0.5124(10)	0.7193(22)	0.089(12)
C(61)	−0.0193(20)	−0.3429(15)	0.7087(26)	0.071(10)
C(62)	0.0744(14)	−0.3725(11)	0.7465(20)	0.068(10)
C(63)	0.1424(14)	−0.3471(11)	0.6805(20)	0.095(11)
C(64)	0.2158(14)	−0.3823(11)	0.6968(20)	0.090(11)
C(65)	0.2212(14)	−0.4430(11)	0.7792(20)	0.088(12)
C(66)	0.1532(14)	−0.4685(11)	0.8453(20)	0.107(14)
C(67)	0.0798(14)	−0.4332(11)	0.8289(20)	0.082(11)
C(71)	−0.2106(21)	−0.3237(15)	0.5535(28)	0.073(9)
C(72)	−0.1970(14)	−0.2443(8)	0.5461(20)	0.066(9)
C(73)	−0.2166(14)	−0.2070(8)	0.4303(20)	0.047(8)
C(74)	−0.2056(14)	−0.1331(8)	0.4199(20)	0.065(9)
C(75)	−0.1748(14)	−0.0966(8)	0.5253(20)	0.102(13)
C(76)	−0.1552(14)	−0.1339(8)	0.6410(20)	0.092(12)
C(77)	−0.1662(14)	−0.2078(8)	0.6514(20)	0.087(11)

Table 6 (continued)

Atom	x	y	z	U_{iso} or U_{eq}
C(211)	0.4776(19)	−0.0776(13)	0.4144(23)	0.051(8)
C(212)	0.4879(18)	−0.1189(10)	0.5365(16)	0.058(9)
C(213)	0.4056(18)	−0.1569(10)	0.5749(16)	0.067(10)
C(214)	0.4202(18)	−0.1912(10)	0.6930(16)	0.076(10)
C(215)	0.5171(18)	−0.1874(10)	0.7728(16)	0.126(15)
C(216)	0.5994(18)	−0.1493(10)	0.7343(16)	0.170(19)
C(217)	0.5848(18)	−0.1151(10)	0.6162(16)	0.112(14)
C(221)	0.4776(20)	−0.1960(14)	0.3012(24)	0.058(8)
C(222)	0.4544(14)	−0.2391(8)	0.1944(14)	0.043(7)
C(223)	0.3588(14)	−0.2552(8)	0.1088(14)	0.066(9)
C(224)	0.3387(14)	−0.2962(8)	0.0118(14)	0.074(10)
C(225)	0.4142(14)	−0.3211(8)	0.0005(14)	0.080(10)
C(226)	0.5098(14)	−0.3050(8)	0.0861(14)	0.089(11)
C(227)	0.5299(14)	−0.2640(8)	0.1831(14)	0.079(10)
C(231)	0.4322(21)	−0.0690(15)	0.1500(27)	0.065(9)
C(232)	0.5431(11)	−0.0367(10)	0.1580(17)	0.051(8)
C(233)	0.5914(11)	0.0282(10)	0.2125(17)	0.070(10)
C(234)	0.6912(11)	0.0612(10)	0.2202(17)	0.079(10)
C(235)	0.7425(11)	0.0294(10)	0.1735(17)	0.080(11)
C(236)	0.6941(11)	−0.0355(10)	0.1190(17)	0.083(10)
C(237)	0.5944(11)	−0.0685(10)	0.1112(17)	0.056(8)
H(1)	0.09301	−0.23459	0.40726	0.08
H(2)	−0.06109	−0.21329	0.31336	0.08

of the silver-ruthenium cluster $[Ag_2Ru_4(\mu_3\text{-}H)_2(CO)_{12}\{P(CH_2Ph)_3\}_2]$ (X) (0.19 g, 37%).

Crystal structure analyses of the clusters $[Cu_2Ru_4(\mu_3\text{-}H)_2(CO)_{12}\{\mu\text{-}P(CH_2Ph)_2(\eta^2\text{-}CH_2Ph)\}]$ (VIII) and $[Cu_2Ru_4(\mu_3\text{-}H)_2(CO)_{12}\{P(CH_2Ph)_3\}_2]$ (IX)

Suitable crystals of VIII and IX were grown from dichloromethane/diethyl ether/light petroleum mixtures by slow layer diffusion at −20 °C.

Crystal data for VIII · $(0.5CH_2Cl_2)$: $(C_{33}H_{23}O_{12}PCu_2Ru_4) \cdot (0.5CH_2Cl_2)$, M = 1216.1, triclinic, space group $P\bar{1}$ (no. 2), a 14.344(3), b 12.235(3), c 11.844(2) Å, α 108.91(2), β 94.70(2), γ 96.08(2)°, U 1940.37 Å^3, $Z = 2$, D_c 2.08 g cm^{-3}, $F(000)$ = 1174. A red crystal of size 0.29 × 0.21 × 0.35 mm, μ(Mo-K_α) = 26.1 cm^{-1}, was used for the data collection.

Crystal data for IX: $C_{54}H_{44}O_{12}P_2Cu_2Ru_4$, M = 1478.0, triclinic, space group $P\bar{1}$ (no. 2), a 14.748(3), b 19.583(4), c 11.636(2) Å, α 79.99(1), β 110.33(3), γ 107.48(3)°, U 2996.76 Å^3, $Z = 2$, D_c 1.64 g cm^{-3}, $F(000) = 1456$. A red crystal of size 0.21 × 0.24 × 0.32 mm, μ(Mo-K_α) 16.9 cm^{-1}, was used for the data collection.

Data collection. Data were collected for both compounds in the θ-range 3–25°, with scan widths of 0.80° (VIII) and 0.90° (IX), by the procedure described previously [27]. Equivalent reflections were merged to give 4696 (VIII) and 3132 (IX) data with $I/\sigma(I) > 3.0$. Absorption corrections were applied to the data after initial refinement with isotropic thermal parameters for all atoms except the hydrido ligands [28].

Structure solution and refinement [29]. In each case, the coordinates of the four ruthenium atoms were deduced from Patterson syntheses and the remaining non-hy-

drogen atoms were located from subsequent difference-Fourier syntheses. For VIII, the hydrogen atoms on the coordinated benzyl group (both on the ring and the methylene group) were located in a difference-Fourier synthesis calculated using data with $\sin\theta < 0.35$. These were included in the structure factor calculations, with thermal factors of 0.08 Å^2, but their parameters were not refined. The dichloromethane molecule in the structure of VIII had the two chlorine atoms related by an inversion centre with two half methylene carbon atoms disordered across this point. The remaining hydrogen atoms on the organic groups and all organic hydrogen atoms for IX were included in geometrically idealised positions and were constrained to 'ride' on the relevant carbon atoms with common group isotropic thermal parameters of 0.08 Å^2 (VIII) and 0.10 Å^2 (IX), which were not refined. It was not possible to locate the hydrido ligands in difference-Fourier maps for either compound, but their positions were deduced from potential energy minima calculations [30]. They were not included in structure factor calculations. For VIII, all of the non-hydrogen atoms were assigned anisotropic thermal parameters in the final cycles of full-matrix refinement which converged at $R = 0.0463$ and $R' = 0.0471$, with weights of $w = 1/\sigma^2(F_o)$ assigned to the individual reflections. For IX, the six metal atoms and the two phosphorus atoms were assigned anisotropic thermal parameters in the final cycles of full-matrix refinement which converged at $R = 0.0697$ and $R' = 0.0672$, with weights of $w = 1/\sigma^2(F_o)$ assigned to the individual reflections. The final atomic coordinates and equivalent isotropic thermal parameters for VIII and IX are given in Tables 5 and 6, respectively. Tables of observed and calculated structure factors are available from the authors.

Acknowledgements

We thank Drs. O.W. Howarth and E. Curzon for recording a number of 400 MHz NMR spectra, the S.E.R.C. for a studentship (P.J.M.) and a Research Fellowship (H.R.P.), and Johnson Matthey Ltd. for a generous loan of silver and ruthenium salts.

References

1 Part XIII. S.S.D. Brown, I.D. Salter, T. Adatia, and M. McPartlin, J. Chem. Soc., Dalton Trans., (1990) 799.
2 M.J. Freeman, A.G. Orpen, and I.D. Salter, J. Chem. Soc., Dalton Trans., (1987) 379.
3 P.J. McCarthy, I.D. Salter, and V. Šik, J. Organomet. Chem., 344 (1988) 411.
4 S.S.D. Brown, I.D. Salter, and B.M. Smith, J. Chem. Soc., Chem. Commun., (1985) 1439.
5 C.J. Brown, P.J. McCarthy, and I.D. Salter, unpublished results.
6 T. Adatia, P.J. McCarthy, M. McPartlin, M. Rizza, and I.D. Salter, J. Chem. Soc., Chem. Commun., (1988) 1106.
7 C.A. Tolman, Chem. Rev., 77 (1977) 313.
8 P.J. McCarthy, M. McPartlin, H.R. Powell, and I.D. Salter, J. Chem. Soc., Chem. Commun., (1989) 395.
9 P.J. McCarthy, I.D. Salter, K.P. Armstrong, M. McPartlin, and H.R. Powell, J. Organomet. Chem., 377 (1989) C73.
10 S.S.D. Brown, I.D. Salter, and L. Toupet, J. Chem. Soc., Dalton Trans., (1988) 757.
11 S.S.D. Brown, I.D. Salter, A.J. Dent, G.F.M. Kitchen, A.G. Orpen, P.A. Bates, and M.B. Hursthouse, J. Chem. Soc., Dalton Trans., (1989) 1227.
12 I.D. Salter, Adv. Organomet. Chem., 29 (1989) 249.

13 For example, I.D. Salter, Adv. Dynamic Stereochem., 2 (1988) 57; K.P. Hall and D.M.P. Mingos, Prog. Inorg. Chem. 32 (1984) 237; D.G. Evans and D.M.P. Mingos, J. Organomet. Chem., 232 (1982) 171; and references cited therein.
14 G.B. Ansell, M.A. Modrick, and J.S. Bradley, Acta Crystallogr., C, 40 (1984) 365; P.G. Jones, ibid., 42 (1986) 1099.
15 M.J. Freeman, A.G. Orpen, and I.D. Salter, J. Chem. Soc., Dalton Trans., (1987) 1001.
16 C.P. Blaxill, S.S.D. Brown, J.C. Frankland, I.D. Salter, and V. Šik, J. Chem. Soc., Dalton Trans., (1989) 2039.
17 R.A. Brice, S.C. Pearse, I.D. Salter, and K. Henrick, J. Chem. Soc., Dalton Trans., (1986) 2181.
18 S.S.D. Brown, P.J. McCarthy, I.D. Salter, P.A. Bates, M.B. Hursthouse, I.J. Colquhoun, W. McFarlane, and M. Murray, J. Chem. Soc., Dalton Trans., (1988) 2787.
19 S.S.D. Brown, S. Hudson, I.D. Salter, and M. McPartlin, J. Chem. Soc., Dalton Trans., (1987) 1967.
20 For example, W.E. Lindsell, N.M. Walker, and A.S.F. Boyd, J. Chem. Soc., Dalton Trans., (1988) 675; M. McPartlin, and W.J.H. Nelson, J. Chem. Soc., Dalton Trans., (1986) 1557; J. Pursiainen, T.A. Pakkanen, B.T. Heaton, C. Serengi, and R.G. Goodfellow, J. Chem. Soc., Dalton Trans., (1986) 681; B.F.G. Johnson and R.E. Benfield in B.F.G. Johnson (Ed.), Transition Metal Clusters, Wiley, New York, 1980, Ch. 7; E. Band and E.L. Muetterties, Chem. Rev., 78 (1978) 639; J. Evans, Adv. Organomet. Chem., 16 (1977) 319; and references cited therein.
21 D.M.P. Mingos, Polyhedron, 3 (1984) 1289.
22 S.S.D. Brown, I.D. Salter, V. Šik, I.J. Colquhoun, W. McFarlane, P.A. Bates, M.B. Hursthouse, and M. Murray, J. Chem. Soc., Dalton Trans., (1988) 2177.
23 I.D. Salter, unpublished results.
24 S.S.D. Brown and I.D. Salter, Organomet. Synth., 4 (1988) 241.
25 G.J. Kubas, Inorg. Synth., 19 (1979) 90.
26 S.S.D. Brown and I.D. Salter, Organomet. Synth., 3 (1986) 315.
27 M.K. Cooper, P.J. Guerney, and McPartlin, J. Chem. Soc., Dalton Trans., (1982) 757.
28 N. Walker and D. Stuart, Acta Crystallogr., A, 39 (1983) 158.
29 G.M. Sheldrick, SHELX 76 program for crystal structure determination, University of Cambridge, 1976.
30 A.G. Orpen, J. Chem. Soc., Dalton Trans., (1980) 2509.